

Efficient Transmission in the Millimeter Waves 28 GHz Outdoor Channel Using Spatial Multiple Access (SMA)

Said E. El-Khamy¹, Hassan M. Elragal¹ and Remon Polus¹

¹Electrical Engineering Department, Alexandria University, Alexandria, Egypt

Received 30 Apr. 2020, Revised 9 Sep. 2020, Accepted 13 Nov. 2020, Published 1 Jan. 2021

Abstract: Non-Orthogonal Multiple Access (NOMA) is considered as one of the key technologies for the fifth generation (5G) of the cellular networks. However, due to the complexity of the Successive Interference, spatial multiple access (SMA) technique – based on using spatial modulation for multiple antenna systems – was proposed to avoid the use of successive interference cancellation. On the other hand, millimeter waves band is a promising band for 5G. This is mainly because the traditional microwave band is currently fully crowded. In this paper we investigate efficient transmission in the millimeter waves 28 GHz Outdoor Channel Using Spatial Multiple Access (SMA). Two ray fluctuating model (TRF) is used in the performance analysis for millimeter waves, as well as the limiting case of the Rayleigh channel. Analytical and simulation results show the performance of SMA over millimeter waves. Finally; the performance is shown to be improved over the more complicated NOMA with SIC.

Keywords: NOMA, Spatial Modulation , Millimeter Waves

1. INTRODUCTION

One of the goals of the fifth generation (5G) is to enable large numbers of devices to be connected with large bandwidth [1]. To meet this requirement, Non-Orthogonal Multiple Access (NOMA) is considered as the multiple access scheme for this generation. However, traditional schemes such as Power-domain NOMA [2] or Code- Domain NOMA [3, 4] requires complex receivers such as Successive Interference Cancellation (SIC) or message passing algorithm (MPA) respectively.

Spatial modulation is a proposed technique in order to increase the spectral efficiency of MIMO systems. Basically, it divides information bits into two groups; the 1st one is responsible for selection of transmit antenna based on space shift keying (SSK) mapping. Whereas, the other group of bits are modulation by M-ary scheme and transmitted via the selected antenna. Fig 1. Illustrates the spatial modulation

Inspired by Spatial modulation [5] and In order to avoid implementation of such complex receivers, spatial multiple access (SMA) was proposed in [6]. It allocates different users in different domain as shown in Figure 1. , One user's data is responsible for antenna selection (spatial domain) and the other user's data is transmitted via the selected antenna.

At the receiver side, it tends to use either maximal ratio combining (MRC) or maximal likelihood (ML) as a receiver. In addition, this scheme limits the number of operating RF chain to only one. This leads to archive a higher increase in the energy efficiency (EE) of the system. However, this techniques provides a fixed data rate of each user.

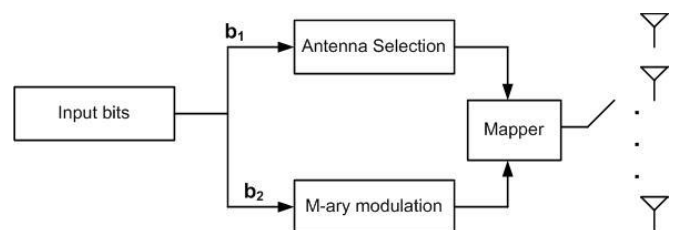


Figure 1. Spatial modulation technique

The millimeter-waves band is a candidate for 5G deployment due to spectrum scarcity in the traditional microwave bands. The 28 GHz band is considered for an initial deployment of mm-waves cellular, given their relatively lower frequency within the mm-waves range which leads to lower attenuation [7].

In this paper, SMA scheme is investigated with the study of its performance under the 28 GHz outdoor channel. Analytical average bit error probability (ABEP) expressions are evaluated and validated by simulations

using the 28 GHz channel. Finally, the performance is compared with the power domain NOMA.

The rest of paper is organized as follows. In section 2, system model is described SMA scheme is presented. In section 3, the performance analysis of the SMA system is discussed in terms of in terms of the ABER. Section 4 shows the simulation results to verify the analytical expression. Concluding remarks are shown in Section 5.

2. SYSTEM MODEL AND CHANNEL MODEL

A. System model

We consider a downlink system consists of a base station (BS) equipped with multiple transmit antennas N_t and serving two users' equipment (UE). Each UE is equipped with N_r receiving antennas. Let the bits of UE-1 (b_1) is transmitted via space shift keying where antenna j is used for transmission. The selection process is based on SSK modulation for b_1 and the data of UE-2 (b_2) is transmitted via M-ary modulation. In that case UE-1 is called the Spatial Modulation user (SM user) and UE-2 is called M-ary user as illustrated in Fig 2.

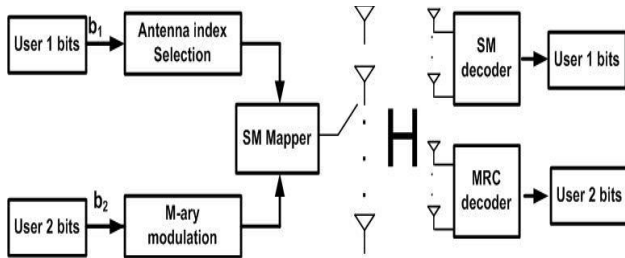


Figure 2. Spatial Multiple Access scheme

The transmitted vector can be written as

$$x = \begin{bmatrix} 0 & 0 & \dots & \underbrace{f_{M\text{-ary}}(b_2)}_{j^{\text{th}} \text{ position}} & \dots & 0 & 0 \end{bmatrix}^T \quad (1)$$

Where

- the j^{th} position depends on SSK mapping of SM user's bits
- $f_{M\text{-ary}}(b_2)$: the M-ary mapping of M-ary user's bits

Table 1 illustrates the mapping operation of the SMA using $N_t = 2$ & PSK - 4. It is clear that if the SM bit = 0; then antenna 1 is selected for transmission, otherwise antenna 2 is used. The transmitted symbol over the selected antenna depends on the PSK - 4 constellation mapping.

Table 2. SMA mapping $N_t = 2$ & PSK - 4

Bits of M-ary user	Bits of SM user	x^T
00	0	$\frac{1}{\sqrt{2}}[1 + j \ 0]$
01	0	$\frac{1}{\sqrt{2}}[-1 + j \ 0]$
11	0	$\frac{1}{\sqrt{2}}[-1 - j \ 0]$
10	0	$\frac{1}{\sqrt{2}}[1 - j \ 0]$
00	1	$\frac{1}{\sqrt{2}}[0 \ 1 + j]$
01	1	$\frac{1}{\sqrt{2}}[0 \ -1 + j]$
11	1	$\frac{1}{\sqrt{2}}[0 \ -1 - j]$
10	1	$\frac{1}{\sqrt{2}}[0 \ 1 - j]$

B. Millimeter waves model

The multipath fading channel model for 28 GHz is the Fluctuating Two-Ray (FTR) fading [8]. It consists of two fluctuating components plus random phase and diffuse components. It arose as the generalization of the two-wave with diffuse power (TWDP) fading model proposed by in [9]. The FTR fading distribution provides a much better fit than Ricean fading to the 28 GHz field measurements results in[10].

In FTR model, Assume the complex baseband receive signal as

$$V_r = \sqrt{\zeta}V_1e^{j\varphi_1} + \sqrt{\zeta}V_2e^{j\varphi_2} + X + jY \quad (2)$$

Where $V_n e^{j\varphi_n}$ represents the n-th component with constant amplitude V_n and uniformly distributed phase φ_1 . $X + jY$ is a complex Gaussian random variable with $N(0, \sigma^2)$ which represents the diffuse received signal component.

The FTR model is defined by the following three parameters

$$k = \frac{V_1^2 + V_2^2}{2\sigma^2} \quad (3)$$

$$\Delta = \frac{2V_1V_2}{V_1^2 + V_2^2} \quad (4)$$



$\sqrt{\zeta}$ is a Gamma distributed random variable and has the following probability density function

$$f_{\zeta}(x) = \frac{2m^m x^{(2m-1)}}{\Gamma(m)} e^{-mx^2} \quad (5)$$

k represents the ratio of the average power of the dominant components to the power of the remaining diffuse multipath. Δ represents the similarity between the received powers from the dominant components and it ranges from zero to one.

The FTR fading model is suitable for many propagation channels. Table 3 summarizes the relationship between FTR model and classical fading channel models (Rayleigh, Rician and Nakagami- m).

Table 3. The relationship between FTR model parameters and classical fading channel

Fading Channel	FTR model parameters (Δ, k, m)
Rayleigh	$\Delta = 0, k \rightarrow \infty, m = 1$
Ricean k	$\Delta = 0, k = k, m \rightarrow \infty$
Nakagami m	$\Delta = 0, k \rightarrow \infty, m = m$

The pdf and CDF of the received SNR for multiple branch receiver for this model can be found in [11].

Fig 3 shows the PDF of The FTR model for different values of m, Δ & k for $N_r = 1$. For larger values of k & $\Delta \rightarrow 1$, the PDF pronounces bimodality. As m decreases, such bimodality decreases. Fig 4. Shows the PDF of the received SNR for different value of N_r for FTR model parameters: $m = 5, \Delta = 0.3$ & $k = 15$

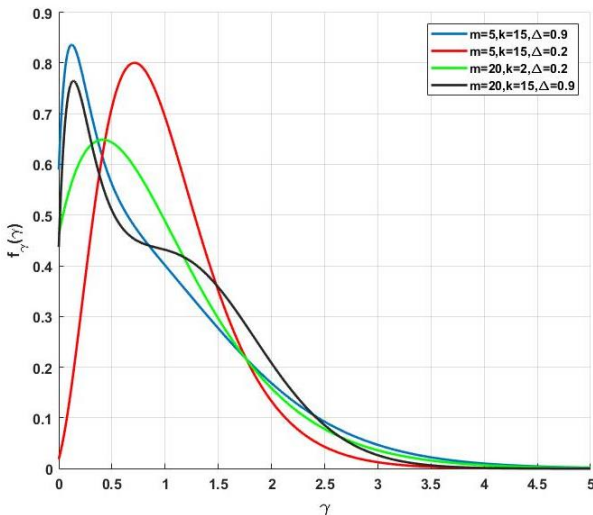


Figure 3. The FTR model PDF for different values m, Δ & k

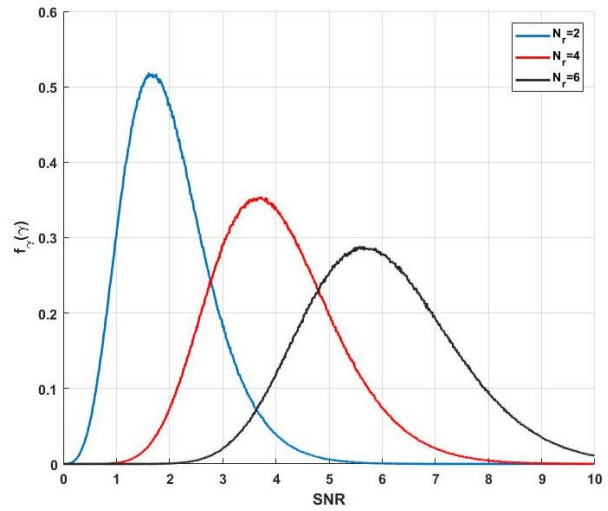


Figure 4. The FTR model PDF for different values of N_r for $m = 5, \Delta = 0.3$ and $k = 15$

C. Detection

The received signal vector after the channel is given by

$$\mathbf{y} = \sqrt{\rho} \mathbf{H} \mathbf{x}_n + \boldsymbol{\eta} \quad (6)$$

Where $\sqrt{\rho}$ represents the transmitted energy, \mathbf{H} is the fading channel matrix $\mathbf{H} \in \mathbb{C}^{N_r \times N_t}$. $\boldsymbol{\eta}$ is the additive white Gaussian noise (AWGN) vector $\boldsymbol{\eta} \in \mathbb{C}^{N_r \times 1}$.

Since only one transmit antenna is activated; the received vector can be written as

$$\mathbf{y} = \sqrt{\rho} \mathbf{h}_j x_n + \boldsymbol{\eta} \quad (7)$$

1) *SM user*: since the data of UE-1 is transmitted via th antenna index. The function of the detector is to obtain which antenna index is used for transmission. The optimal detector is ML which is given by [12]

$$\hat{j} = \arg \min_j \| \mathbf{y} - \sqrt{\rho} \mathbf{h}_j x_n \|^2 \quad (8)$$

2) *M-ary user*: since the data of UE-2 is transmitted via M-ary modulation and it is equipped with N_r antennas for reception Hence, it implements a maximal likelihood (ML) receiver with Maximal ratio combining (MRC) based detection.

$$\hat{x}_n = \arg \min_n \| \mathbf{y} - \sqrt{\rho} \mathbf{h}_j x_n \|^2 \quad (9)$$



3. PERFORMANCE ANALYSIS

1) *SM user*: For SM user, the average bit error probability (ABEP) is calculated via the upper bound technique which is given by

$$ABER = \frac{1}{N_t \log_2 N_t} \sum_{t_1=1}^{N_t} \sum_{t_2=1}^{N_t} N_H(t_1, t_2) PER(t_1 \rightarrow t_2) \quad (10)$$

Where $N_H(t_1, t_2)$ is the hamming distance between the antenna indexes t_1 and t_2 and $PER(t_1 \rightarrow t_2)$ represents the pairwise error probability of antenna indexes t_1 and t_2 . Using the moment generating function (MGF) approach [13], the $PER(t_1 \rightarrow t_2)$ can be formulated as

$$PER(t_1 \rightarrow t_2) = \frac{1}{\pi} \int_0^{\pi/2} \prod_{l=1}^{N_r} M_{t_1, t_2} \left(\frac{E_m}{4N_o} \frac{1}{2 \sin^2 \theta} \right) d\theta \quad (11)$$

Where $\frac{E_m}{N_o}$ is the energy to noise spectral density ratio and $M_{t_1, t_2}(\cdot)$ is the MGF of the fading channel.

2) *M-ary user*: For M-ary user, the BER for MPSK can be written over AWGN [14] as

$$P_b(\gamma) = \frac{1}{\pi \times \log_2 M} \int_0^{(M-1)\pi/M} \exp\left(\frac{-g\gamma}{\sin^2 \theta}\right) d\theta \quad (12)$$

Where $g = \sin^2(\pi/M)$

The ABEP of the M-ary user is obtained by averaging conditional BEP over the instantaneous SNR

$$ABEP = \int_0^\infty P_b(\gamma) p_\gamma(\gamma) d\gamma \quad (13)$$

WHERE $p_\gamma(\gamma)$ IS THE PDF OF THE RECEIVED SNR γ FOR $1 \times N_r$ CHANNEL GIVEN IN [10].

4. SIMULATION RESULTS

Fig 5. shows the BER vs. different values of SNR for the SM user under the FTR millimeter waves channel model with parameters $\Delta = 0, K = 100$ and $m = 1$ for two cases of N_t and N_r . The results of FTR model matches the results of analytical expression BER performance of SM user under Rayleigh channel found in [12] which confirms the assumptions in Table 2 that FTR model reduces to Rayleigh channel when $\Delta = 0, K \rightarrow \infty$ and $m = 1$.

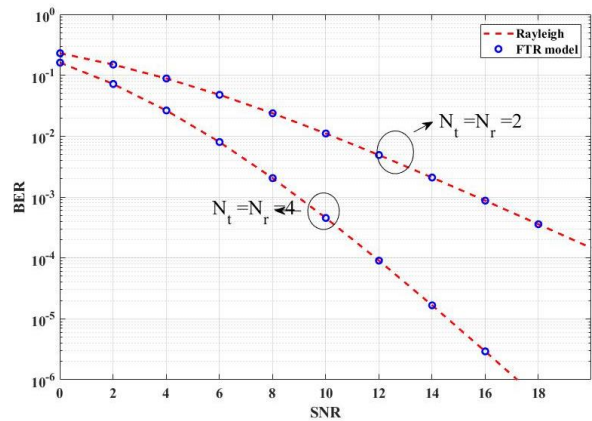


Figure 5. BER vs. SNR for SM user under Rayleigh and FTR model parameters $\Delta = 0, K = 100$ and $m = 1$

Fig 6. Shows the average BER for SM user under FTR model with ($m = 2, k = 10$ and $\Delta = 0.8$) with $N_r = 2$. And different number of transmit antennas. This ABER increases as the number of transmit antennas increases. This is because increasing the number of transmit antennas means increasing the spatial constellation size thus increases the occurrence of error.

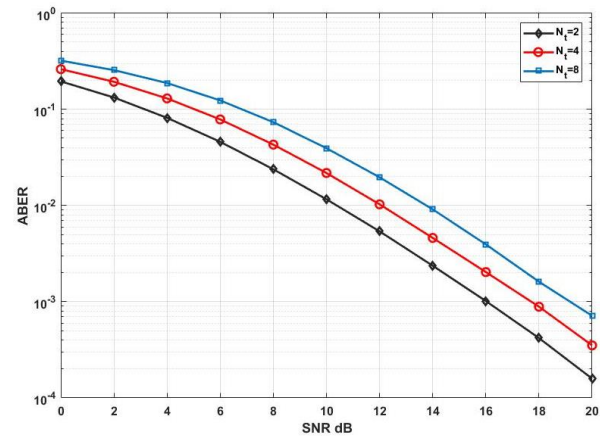


Figure 6. Average BER vs. SNR for the SM user under the FTR model ($m = 2, k = 10; \Delta = 0.8$) with $N_r = 2$

Fig 7 illustrates the BER performance of M-ary user under different values of k parameter & N_r using 4-PSK as the modulation order with FTR millimeters channel model ($\Delta = 0.9$, and $m = 2$). It is clear that as k increases, the BER performance decreases. This is because when k increases, it indicates the increase of the average power of the dominant components to the power of the remaining diffuse multipath ones which in turn improves the system performance. In addition, increasing the number of receive antennas at the MRC leads to increase the diversity order with improves the system performance.

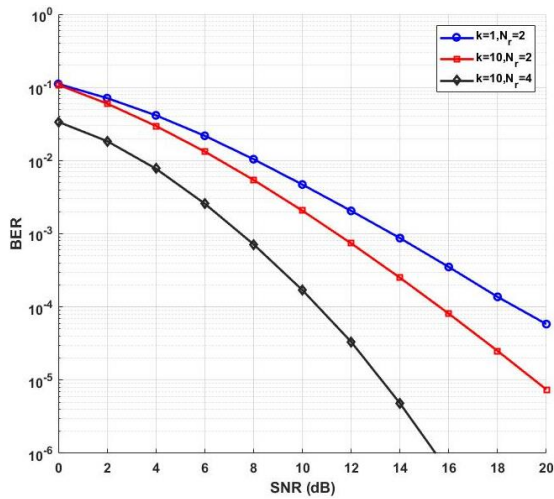


Figure 7 Average BER vs. SNR for the M – ary user under the FTR model ($m = 2$ and $\Delta = 0.9$) with different N_r

Fig.8 compares between power domain NOMA and SMANOMA under the same propagation channel. $N_t = N_r = 2$. The power allocation coefficients for NOMA users are chosen as $a_1 = 0.25$ and $a_2 = 0.75$. It is clear that SMA-NOMA outperforms power domain NOMA using SIC at the receiver

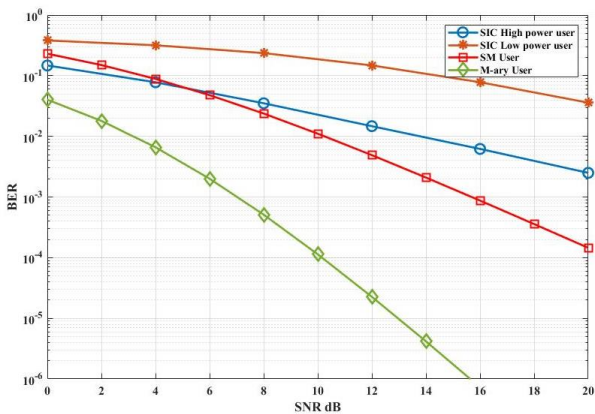


Figure 8. BER vs. SNR between power domain NOMA and SMA NOMA

5. CONCLUSION

In this paper, the spatial multiple access (SMA) is considered as a multiple access technique for the millimeter waves 28 GHz Outdoor Channel. The analytical ABEP expressions are evaluated in terms of the MGF of the channel. Simulation results reveal that SMA-NOMA is better than power domain NOMA for multi- antennas system. In addition, the results verified the relationship between FTR model and other fading channels. The results also demonstrated the effect of varying FTR models on the performance of the system.

REFERENCES

- [1] M. Agiwal, A. Roy, and N. Saxena, "Next generation 5G wireless networks: A comprehensive survey," *IEEE Communications Surveys & Tutorials*, vol. 18, no. 3, pp. 1617-1655, 2016.
- [2] S. R. Islam, N. Avazov, O. A. Dobre, and K.-S. Kwak, "Power-domain non-orthogonal multiple access (NOMA) in 5G systems: Potentials and challenges," *IEEE Communications Surveys & Tutorials*, vol. 19, no. 2, pp. 721-742, 2017.
- [3] R. Hoshyar, F. P. Wathan, and R. Tafazolli, "Novel low-density signature for synchronous CDMA systems over AWGN channel," *IEEE Transactions on Signal Processing*, vol. 56, no. 4, pp. 1616-1626, 2008.
- [4] H. Nikopour and H. Baligh, "Sparse code multiple access," in *Personal Indoor and Mobile Radio Communications (PIMRC), 2013 IEEE 24th International Symposium on*, 2013, pp. 332-336: IEEE.
- [5] R. Mesleh, H. Haas, S. Sinanovic, C. W. Ahn, and S. Yun, "Spatial modulation," *IEEE Transactions on Vehicular Technology*, vol. 57, no. 4, p. 2228, 2008.
- [6] C. Zhong, X. Hu, X. Chen, D. W. K. Ng, and Z. Zhang, "Spatial Modulation Assisted Multi-Antenna Non-Orthogonal Multiple Access," *IEEE Wireless Communications*, vol. 25, no. 2, pp. 61-67, 2018.
- [7] S. Rangan, T. S. Rappaport, and E. Erkip, "Millimeter-wave cellular wireless networks: Potentials and challenges," *Proceedings of the IEEE*, vol. 102, no. 3, pp. 366-385, 2014.
- [8] J. M. Romero-Jerez, F. J. Lopez-Martinez, J. F. Paris, and A. Goldsmith, "The fluctuating two-ray fading model for mmWave communications," in *2016 IEEE Globecom Workshops (GC Wkshps)*, 2016, pp. 1-6: IEEE.
- [9] G. D. Durgin, T. S. Rappaport, and D. A. De Wolf, "New analytical models and probability density functions for fading in wireless communications," *IEEE Transactions on Communications*, vol. 50, no. 6, pp. 1005-1015, 2002.
- [10] M. K. Samimi, G. R. MacCartney, S. Sun, and T. S. Rappaport, "28 GHz millimeter-wave ultrawideband small-scale fading models in wireless channels," in *2016 IEEE 83rd Vehicular Technology Conference (VTC Spring)*, 2016, pp. 1-6: IEEE.
- [11] M. Olyaei, M. Eslami, and J. Haghghat, "Performance of maximum ratio combining of fluctuating two - ray (FTR) mmWave channels for 5G and beyond communications," *Transactions on Emerging Telecommunications Technologies*, vol. 30, no. 10, p. e3601, 2019.
- [12] J. Jeganathan, A. Ghrayeb, and L. Szczecinski, "Generalized space shift keying modulation for MIMO channels," in *Personal, Indoor and Mobile Radio Communications, 2008. PIMRC 2008. IEEE 19th International Symposium on*, 2008, pp. 1-5: IEEE.
- [13] M. Di Renzo and H. Haas, "Bit error probability of space modulation over Nakagami-m fading: Asymptotic analysis," *IEEE Communications Letters*, vol. 15, no. 10, pp. 1026-1028, 2011.
- [14] M. K. Simon and M.-S. Alouini, *Digital communication over fading channels*. John Wiley & Sons, 2005.



Said E. El-Khamy received the B.Sc. (Honors) and M.Sc. degrees from Alexandria University, Alexandria, Egypt, in 1965 and 1967 respectively, and the Ph.D. degree from the University of Massachusetts, Amherst, USA, in 1971. He joined the teaching staff of the Department of Electrical Engineering, Faculty of Engineering, Alexandria University, Alexandria, Egypt, since 1972 and was appointed



as a Fulltime Professor in 1982 and as the Chairman of the Electrical Engineering Department from September 2000 to September 2003. He is currently an Emeritus Professor.

Prof. El-Khamy has published more than three hundreds scientific papers in national and international conferences and journals and took part in the organization of many local and international conferences. His Current research areas of interest include Spread-Spectrum Techniques, Mobile and Personal Communications, Wave Propagation in different media, Smart Antenna Arrays, Space-Time Coding, Modern Signal Processing Techniques and their applications in Image Processing, Communication Systems, Antenna design and Wave Propagation problems.

Prof. El-Khamy is a Fellow member of the IEEE since 1999. He received many prestigious national and international prizes and awards including the State Appreciation Award (Al-Takderia) of Engineering Sciences for 2004, the IEEE R.W.P. King best paper award of the Antennas and Propagation Society of IEEE, in 1980, the A. Schuman's-Jordan's award for Engineering Research in 1982, and the most cited paper award from Digital Signal Processing Journal in 2008. He is also a Fellow of the Electromagnetics Academy and a member of Tau Beta Pi, Eta Kappa Nu and Sigma Xi.



Hassan M. Elragal received the B.Sc., M.Sc. in Electrical Engineering from Alexandria University, Alexandria, Egypt, in 1991 and 1995 respectively. He received his Ph.D. degree in Electrical Engineering at Southern Methodist University, Dallas, Texas in July 2001. His research interest is in the area of signal processing, fuzzy logic, neural networks, genetic algorithm, particle swarm optimization and their applications.



Remon A. Polus received the B.Sc., in Electrical Engineering from Alexandria University, Alexandria, Egypt, in 2016 where he is currently pursuing the M.Sc. degree. Since 2017, he has been with the Department of Electrical Engineering, Alexandria University, where he is currently a Teacher Assistant. His current research areas include wireless communications, signal processing, and MIMO systems.